Journal of Electroanalytical Chemistry 756 (2015) 171–178

Contents lists available at ScienceDirect

Journal of Electroanalytical Chemistry

journal homepage: www.elsevier.com/locate/jeac

Electrochemical detection of free chlorine at inkjet printed silver electrodes

Milica Jović, Fernando Cortés-Salazar, Andreas Lesch, Véronique Amstutz, Hongyan Bi [1], Hubert H. Girault *

Laboratoire d'Electrochimie Physique et Analytique, École Polytechnique Fédérale de Lausanne — Valais Wallis, CH-1951 Sion, Switzerland

ARTICLE INFO

Article history:
Received 2 July 2015
Received in revised form 15 August 2015
Accepted 18 August 2015
Available online 24 August 2015

Keywords:
Free chlorine detection
Inkjet printing silver electrodes
Linear sweep voltammetry

ABSTRACT

A low-cost, reliable and sensitive electrochemical method for free chlorine analysis in water using inkjet printed silver electrodes is presented. Free chlorine detection was based on linear sweep voltammetry (LSV) analysis of $AgCl/Ag_2O$ films formed over an inkjet printed silver electrode by the spontaneous reaction between silver and free chlorine species (*i.e.* HClO and ClO^-) present in solution. The formation of $AgCl/Ag_2O$ films was studied and characterized by high resolution scanning electron microscopy (HR SEM) and X-ray photoelectron spectroscopy (XPS) techniques. LSV characterization demonstrated a quantitative linear relationship between the amount of $AgCl/Ag_2O$ formed and the concentration of free chlorine in water within a range from 1 to 100 ppm. After optimization of several parameters (*e.g.* scan rate, reaction time, starting potential), lowest detectable free chlorine concentration was 0.4 ppm (by standard addition method), while the limit of detection ($S/N = 3$) was equal to 2 ppm, with a sensitivity of 30 μC/ppm. The validation of the proposed methodology was performed by comparison with the standard *N*,*N*-diethylparaphenylenediamine (DPD) method for analyzing swimming pool water samples. Finally, it was demonstrated that reproducible and disposable silver electrodes could be easily prepared by inkjet printing in a large scale and in any required geometry to fit on-line and on-site free chlorine analyses requirements.

1. Introduction

Free chlorine is a strong oxidizing agent widely used in the treatment of drinking water, swimming pools, waste waters, as well as in paper, food and rubber industries [1,2]. In water treatment, chlorine is usually added either in its gaseous form (Cl_2), or as the sodium or calcium hypochlorite salt, since Cl_2-containing aqueous solutions lead to the formation of hypochlorous acid through the reaction [3]:

$$Cl_2 + H_2O \rightarrow HClO + HCl \quad (1)$$

However, depending on pH, hypochlorite (ClO^-), rather than HClO (or a mixture of both) can be formed, the pK_a of the corresponding acid–base reaction being 7.4. Therefore by definition, the sum of the amounts of HClO and ClO^- present in an aqueous system is called free chlorine. This does not account for the chlorine added, but only to the chlorinated species that still remain after reaction with any oxidizable species (*i.e.* organic or metal species) present in the sample. Commonly, the presence of free chlorine in water is related to the absence of disease-causing organisms and therefore is an indicator of microbiological safety [3–5]. However, an excess of free chlorine may result in irritation and difficulties for breathing, while in abnormal quantities it can cause serious damages to biological systems and lead to atherosclerosis, arthritis and cancer [6–9]. Drinking water has a very low free chlorine concentration limit (*i.e.* 0.2 ppm), while that of swimming pools is higher (*i.e.* 2 to 5 ppm) [9]. Total residual chlorine in water discharge from water treatment plants is usually in the range 0.6 to 1 ppm [10,11]. According to the U.S. Department of Agriculture (USDA), the level of free chlorine in poultry chiller makeup water and in reuse waters should not exceed 50 and 5 ppm, respectively [5]. Therefore, measuring free chlorine content in water is of high relevance for many applications, and the implementation of fast, cheap and sensitive new methodologies for environmental monitoring is well justified.

Common analytical methods, such as colorimetric, spectrophotometric [2,12], chemiluminescence [13], chromatography coupled to mass spectrometry (*i.e.* electrophilic addition to styrene) [1], as well as iodometric and amperometric titrations have been employed to measure the free chlorine content in water [3]. Electrochemical methods have shown to be a good alternative for the analysis of different inorganic and organic species due to their sensitive and rapid response, in addition to their simplicity and their possible on-line operation [14]. In particular, amperometry and potential sweep techniques have been extensively involved in the direct determination of free chlorine using its electrochemical oxidation or reduction properties [15–23]. The

* Corresponding author.
E-mail address: hubert.girault@epfl.ch (H.H. Girault).
[1] Present address: Hongyan Bi International Iberian Nanotechnology Laboratory (INL), Av. Mestre José Veiga, 4715-330 Braga, Portugal.

http://dx.doi.org/10.1016/j.jelechem.2015.08.024
1572-6657/

type of electrode materials used for chlorine analysis include platinum [19,21–25], gold [26,27], glassy carbon [15], graphite [16], CNT composite electrodes [21], poly-melamine modified electrodes [28], AuNPs/PEDOT nanocomposite [29] and poly MnTAPP-nano Au film modified electrodes [30]. However, the determination of free chlorine using inkjet printed silver electrodes has not been reported to date. Stripping voltammetry for chlorine analysis by a system using a silver electrode was mentioned in the patent literature, but no results were shown without clear explanation of the working principle and of the employed apparatus [31]. Recently, inkjet printing of functional devices has attracted a much attention as demonstrated by a growing number of applications, such as the fabrication of disposable, cost-competitive sensors with fast response and low detection limits [32–35].

Although widely used as reference electrode material in electrochemistry, silver is not often used as a working electrode because of its small potential window and chemical lability. Despite these facts, silver still holds advantages for electrochemical studies such as its relatively low price compared to the other noble metals, and, in the present study, its reactivity with chlorinated species and the possibility to prepare reproducible silver electrodes by inkjet printing. Similar approach was mentioned in the study by da Silva et al. [36] for manufacturing Ag/AgCl reference electrodes. The main advantages of using inkjet printed silver electrodes over regular silver electrodes are the following: i) the inkjet printed electrodes are disposable and less expensive than common silver electrodes due to the smaller amount of silver employed, ii) a highly reproducible response can be achieved among different electrodes thanks to the fact that the electrode area is precisely defined by the inkjet printing processes, iii) the fabrication of Ag electrodes by inkjet printing is very flexible in terms of scalability simply by modifying the desired dimensions and geometries in the digital pattern files, and iv) a broad range of solid and flexible substrates is available. These advantages enable the rapid, reliable and affordable production of single or multiplexed, portable and easy-to-use sensors. Herein, an easy-to-perform electrochemical method for the analysis of free chlorine in aqueous media based on the spontaneous reaction of free chlorine with an inkjet printed silver electrode is presented. The presence and concentration of free chlorine species are thus transduced at the silver electrode in the form of an $AgCl/Ag_2O$ film that can be quantitatively analyzed by linear sweep voltammetry (LSV). Silver electrodes were printed on flexible polyimide substrates, allowing for small and portable sensing systems for the analysis of free chlorine in forensic, swimming pool or industrial water samples. After optimization of different parameters, lowest detectable free chlorine concentration was 0.4 ppm (by approximation of calibration curve to $y = 0$), while the limit of detection (S/N = 3) was equal to 2 ppm, with a sensitivity of 30 μC/ppm.

2. Experimental Part

Potassium dihydrogen phosphate (KH_2PO_4) was purchased from Sigma Aldrich, disodium tetraborate decahydrate ($Na_2B_4O_7x10H_2O$) from Fischer Scientific and sodium hydroxide (NaOH) from Fluka. Sodium hypochlorite solution (NaClO, available chlorine 5%) was obtained from ACROS Organics™. All chemicals used were of analytical reagent grade. Aqueous solutions were prepared using ultra pure deionized water (Millipore, 18.4 MΩ cm). Buffer solutions of KH_2PO_4-NaOH (50 mM, pH 5.8), KH_2PO_4-NaOH (50 mM, pH 8) and $Na_2B_4O_7x10\ H_2O$ (50 mM, pH 9) were employed as supporting electrolytes. For the validation of the proposed methodology, commercial disinfectant *Eau de Javel* (2.5% NaClO) and water sample from swimming pool in Lausanne, Switzerland were used and kept in a dark and cold place prior to its analysis. The pH was measured with a conventional pH meter (Metrohm 744). For the readout of the N,N-diethylparaphenylenediamine (DPD) spectrophotometric method, a UV-Visible ChemStation from Agilent Technologies was used.

2.1. Inkjet Printing of Silver Working Electrodes

Silver working electrodes were prepared by using a drop-on-demand inkjet printer (DMP-2831 Dimatix Fujifilm, Santa Clara, CA, USA) and a disposable cartridge (DMC11610 Dimatix Fujifilm, Santa Clara, CA, USA) containing 16 individually addressable nozzles with nominal droplet volumes of 10 pL. All silver patterns were printed over a Kapton HN foil substrate (polyimide (PI); 125 μm-thick; Goodfellow, Huntingdon, England) using a commercial silver ink (EMD5603, Sunchemical, Carlstadt, USA). During printing of the silver layer, the substrate temperature was set to 60 °C in order to promote evaporation of the ink carrier and thus to increase the pattern resolution. After printing, Ag patterns were cured for 30 min at 200 °C with a heating and cooling rate of 1–2 °C/min. Afterwards, an insulating layer was printed over the silver pattern to precisely define the active area of the silver electrode (*i.e.* surface 4 mm^2, Fig. 1). The insulating UV curable ink (EMD6101, Sunchemical, Carlstadt, USA) was simultaneously polymerized by UV exposition with a light guide connected to an Omnicure S2000 mercury UV lamp (Lumen Dynamics, Mississauga, Ontario, Canada) and mounted on the DMP-2831 print head. Printing parameters (cleaning steps, cartridge temperature, waveform, jetting frequency, number of nozzles, etc.) were optimized for both employed inks. Electrical connections were checked with a multimeter, while dimensions and physical characteristics of the printed patterns were investigated by laser-scanning microscopy (LSM) in reflection mode using a Keyence VK 8700 (Keyence, Osaka, Japan). Further characterization of the inkjet printed electrodes before and after the electrochemical detection of free chlorine was performed by high resolution scanning electron microscopy (HR SEM, Merlin Zeiss, Germany) equipped with a Gemini II column and a secondary electron, in-lens detector. Finally, the chemical composition of the $AgCl/Ag_2O$ film surface was investigated by X-ray Photoelectron Spectroscopy, XPS (ESCA KRATOS AXIS ULTRA).

2.2. Electrochemical Detection of Free Chlorine with Silver Printed Electrodes

A 500 ppm free chlorine standard solution was prepared by dilution of a 5% aqueous NaClO stock solution. Other solutions with lower concentrations were freshly prepared by dilution of the 500 ppm standard solution and using a specific pH buffer solution. All solutions were kept in the dark, transported in brown glass bottles and stored at 4 °C. Analyzed free chlorine solutions were in the range from 1 to 100 ppm. Experiments were performed in air at atmospheric pressure conditions and at 21 ± 2 °C. Electrochemical measurements were carried out in a single compartment cell containing a Ag/AgCl (1 M KCl) reference electrode, a platinum wire counter electrode and the inkjet printed silver working electrode. All measurements were performed in a total volume of 10 mL of sample solution. The linear sweep voltammetry (LSV) experiments were carried out with an Autolab potentiostat (PGSTAT128N, Utrecht, Netherlands). The quantification of free chlorine proceeded as follows (*vide infra*): 1) electrode preconditioning, in order to have a completely clean and reduced surface of silver electrode; 2) formation of $AgCl/Ag_2O$ as a result of the reaction between the silver electrode and the present free chlorine, 3) replating of silver and transduction of the voltammetric signal into the free chlorine concentration.

3. Results and Discussion

3.1. Characterization of Inkjet Printed Electrodes

As described above, the silver patterns were constituted of a small square (4 mm^2) linked to a rectangle (20 mm × 1 mm) employed for the electrical connection. A UV curable insulating ink pattern was printed along the rectangle (12 mm × 2 mm) to precisely define the square of active electrode area (Fig. 1b). As seen on the SEM images

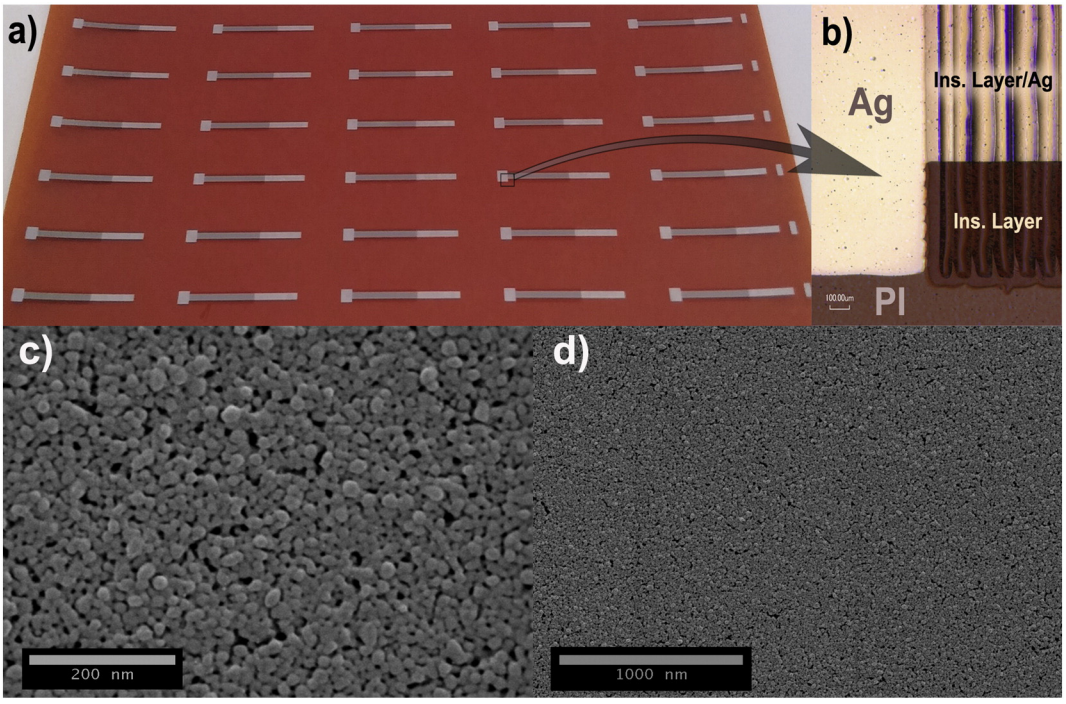

Fig. 1. a) Photograph of a batch of inkjet printed silver electrodes; b) laser–color scanning micrograph and c–d) HR SEM (with magnifications of c) 100 000× and d) 400 000×) of the active area of the inkjet printed Ag electrode.

(Fig. 1c, 1d) the active electrode area consisted of a uniform coverage of densely packed silver clusters. The small voids among the particles observed in Fig. 1c and 1d are most likely due to the incomplete sintering among the silver nanoparticles and the evaporation of volatile organic compounds contained in the ink formulation [37]. A higher magnification image (Fig. 1d) was used for measuring the particle size, which was around 25 nm. Thanks to the present fabrication process, a high reproducibility on the electrode characteristics assured not only a high inter-electrode reproducibility, but also the ability for large-scale production of silver electrodes (Fig. 1a).

3.2. Free Chlorine Detection on Inkjet Printed Silver Electrodes

As shown in Fig. 2, the principle of free chlorine detection using silver electrodes is based on the formation of a $AgCl/Ag_2O$ layer over the silver electrode, as a consequence of the spontaneous reaction between silver and free chlorine species. In a following step, the formed layer can be quantitatively stripped and thus silver replated on the electrode surface by means of cathodic stripping voltammetry. As the amount of oxidized silver is proportional to the concentration of free chlorine and the time of exposure, the quantification of free chlorine can be achieved based on the obtained voltammetric signals.

The surface chemical composition of the bare printed silver electrode and the formed $AgCl/Ag_2O$ layer was investigated by XPS (Table 1). Based on the obtained results, the bare inkjet printed silver electrode was composed of (atomic concentrations): Ag 46.5%, C 37.7% and O 15.8%. Besides silver, electrodes contain oxygen, due to silver oxidation when in contact with air, and carbon (from the silver ink formulation). The O/Ag and C/Ag atomic concentration ratios were 0.34 and 0.81, respectively. However, after reaction with free chlorine there was an evident presence of chlorine at the silver electrode surface, beside of carbon and oxygen. Cl/Ag ratio after reaction with 16 ppm of free chlorine was 0.42, while the O/Ag ratio increased from 0.34 to 0.39. This means that the layer on the silver electrode was preferentially composed of AgCl, but also contained some amount of Ag_2O. Indeed, the formation of AgCl is thermodynamically more favorable than the one of Ag_2O ($\Delta G°_{AgCl} = -109.5$ kJ/mol, $\Delta G°_{Ag2O} = -10.8$ kJ/mol) and can be presented by the following equations:

$$Ag + HClO + H^+ \rightarrow AgC1 + H_2O \quad (2)$$

$$Ag + ClO^- + H_2O \rightarrow AgCl + 2\ OH^- \quad (3)$$

A SEM image of the layer formed on the silver surface is shown in Fig. 3. As a result of the reaction of silver with the 16 ppm free chlorine solution (Fig. 3a), concave-cubical shaped crystals were formed and uniformly distributed over the electrode surface. It has been reported that the concentration of chlorinated species in the solution plays an important role in the final shape of AgCl crystals [34], which is consistent with our observations. It was noticed that with lower free chlorine

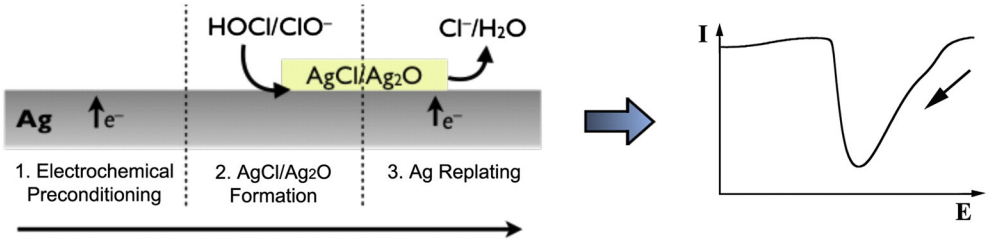

Fig. 2. Principle of detection of free chlorine on inkjet printed silver electrodes; plot of the signal obtained from the third step by LSV.

Table 1
XPS analysis of inkjet printed silver electrodes before and after exposition to a 16 ppm free chlorine solution for 200 s.

Element	Silver electrode	Silver electrode after reaction with 16 ppm free chlorine
	Atomic concentration (%)	
Ag *3d*	46.5	31.1
C *1s*	37.7	43.5
O *1s*	15.8	12.3
Cl *2p*	–	13.1

concentration particles have a concave-cubical structure, while with higher concentration (*ca.* 200 ppm) they have more round shape. Additionally, it was observed that the free chlorine concentration also affects the particle size. For instance, smaller particles were formed with higher free chlorine concentrations (Fig. 3b), which could be explained by the formation of more nucleation sites on the silver electrode. On the other hand, with lower free chlorine concentration there was less nucleation sites formed, but crystal growth stage is more pronounced. Higher concentrations of free chlorine resulted in a removal of the electrode surface from the substrate.

Taking into account the XPS and HR SEM results, special attention has to be paid to the state of the silver working electrode surface, since (electro)chemical oxidation of the silver surface (by air, for instance) could decrease the available electrode area, as well as introduce interferences due to the presence of Ag_2O. For this reason, an electrochemical preconditioning protocol was implemented before each analysis to assure reproducible results (*vide infra*).

3.3. Optimization of Free Chlorine Detection

For the optimization of the free chlorine detection, several parameters were assessed, such as starting potential, electrochemical cleaning, pH and scan rate. Fig. 4 shows the linear sweep voltammogram obtained at the inkjet printed silver electrode in a buffer solution of KH_2PO_4 (50 mM, pH 5.8) within the potential window from 0.3 to −1.1 V *vs.* Ag/AgCl. In the absence of free chlorine species, two reduction peaks are observed. The first peak (peak 1, *i.e.* 0.1 V *vs.* Ag/AgCl) corresponds to the reduction of Ag_2O and has a triangular shape typical for electrochemical processes controlled by surface phenomena (*e.g.* adsorption/desorption), while the second one (peak 2, *i.e.* –0.3 V *vs.* Ag/AgCl) is related to the reduction of dissolved oxygen and has a sigmoidal shape.

When free chlorine species are added to the solution, the signal related to the oxidized silver film overlaps with peak 1, making any quantification difficult. In order to remove this interference, we optimized the starting potential to find a value at which there is no previous oxidation of the silver electrode due to the starting potential. As a result, any

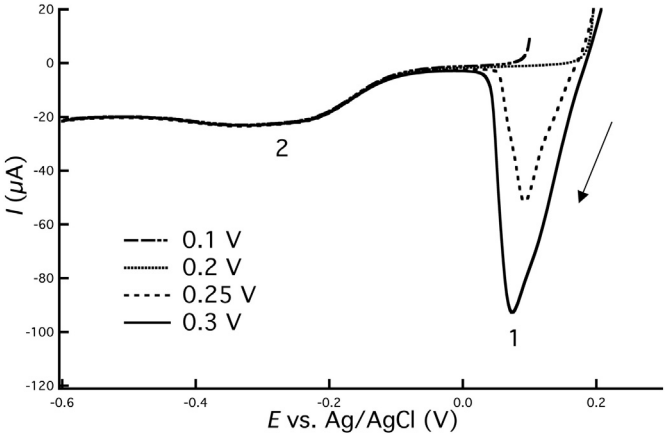

Fig. 4. Linear sweep voltammograms at a inkjet printed silver electrode in a KH_2PO_4 (50 mM, pH 5.8) buffer solution, scan rate 50 mV · s^{-1}, starting potentials: 0.3 V; 0.25 V; 0.2 V and 0.1 V.

recorded signal will rise only from the reaction between silver and free chlorine. When the starting potential was 0.3 V or 0.25 V (Fig. 4) a clear signal associated with the Ag_2O reduction is observed. However, when the starting potential is 0.2 V (Fig. 4), it disappears, meaning that no significant oxidation of the silver electrode will occur previous to the electrochemical experiment. Since less positive starting potentials are not more advantageous for the precision and sensitivity (*e.g.* 0.1 V, Fig. 4), a starting potential of 0.2 V was chosen as the optimal one and used in further experiments.

The reproducibility of electrochemical signals is highly dependent on the state of the electrode before analysis. For instance, electrochemical determinations at mechanically polished electrodes may lack reproducibility and demand time and expertise. As an alternative, electrochemical preconditioning of the working electrode at a given potential value might suppresses the need for mechanical polishing. This is especially relevant in the case of inkjet printed electrodes, as mechanical polishing is not an option due to the fragility of the thin silver layer with applied mechanical force. Therefore, inkjet printed silver electrodes were electrochemically preconditioned by applying a potential of −0.3 V for different time intervals. Based on the LSVs of Fig. 4, this preconditioning potential value was chosen in order to have a completely reduced and clean silver surface. Fig. 5 shows the LSV for a silver electrode in a 16 ppm free chlorine solution without and with electrochemical cleaning at −0.3 V for 15, 30, and 60 s before each analysis. It can be seen that without electrochemical preconditioning, the signal for the same free chlorine concentration is much higher albeit non-reproducible, since the oxidation state of the electrode surface

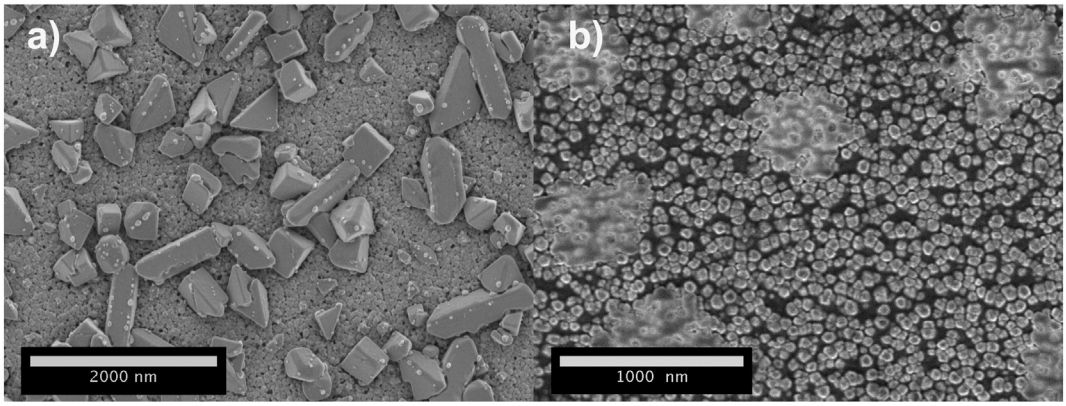

Fig. 3. SEM HR images of inkjet printed silver electrode after reaction with a) 16 ppm (magnification 50000×) and b) 200 ppm free chlorine solution (magnification 100000×).

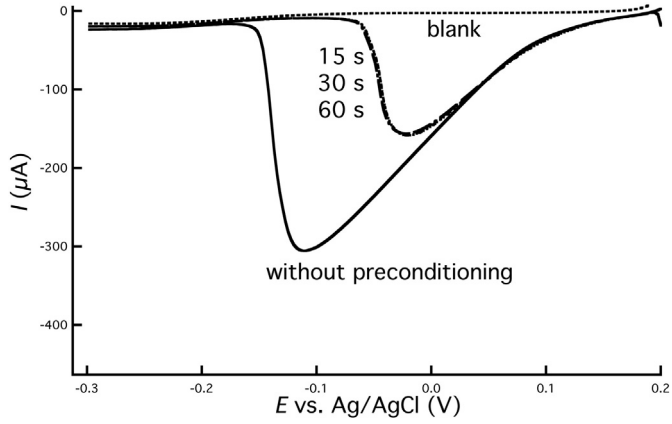

Fig. 5. Linear sweep voltammograms at an inkjet printed silver electrode in the reaction with 16 ppm free chlorine solution (50 mM KH_2PO_4, pH 5.8), with a preconditioning step at −0.3 V for 15, 30, 60 and 90 s. Starting potential 0.2 V, scan rate 100 mV · s^{-1}, reaction time with free chlorine 60 s.

cannot be controlled. With preconditioning at negative potentials to fully reduce the electrode, a reproducible response is observed for each cleaning time, validating thus this methodology. Moreover, this experiment also demonstrates the possibility of multiple usages of the silver electrodes. Since there was no significant difference between the different preconditioning times examined, a preconditioning time of 15 s was employed in further experiments.

The influence of the scan rate on the detection of free chlorine at silver electrode was also studied. The LSVs at different scan rates are shown in Fig. 6, while the peak area as a function of the scan rate is shown in the inset a). It was found that the peak area is linearly proportional to the scan rate in the range of 10 to 100 mV · s^{-1} ($r^2 = 0.9948$) and that charge is constant with the scan rate, inset b). This indicates that the electrode process is mainly controlled by surface phenomena, such as the stripping of the $AgCl/Ag_2O$ film and replating of silver. The observed shift of the peak potentials towards more cathodic values with increasing scan rate is due to the limited kinetics of the electron-transfer process at the electrode surface. In further experiments 100 mV · s^{-1} was employed as scan rate.

From Fig. 6, it became clear that the reduction peak (peak 1, *i.e.* 0.1 V *vs.* Ag/AgCl) actually consisted of two close signals, which correspond most likely to the reduction of AgCl and Ag_2O (standard reduction potentials of AgCl and Ag_2O are 0.22 V and 0.34 V *vs.* SHE, respectively). The signal from the AgCl reduction is higher, as the formation of AgCl is thermodynamically more favorable than Ag_2O (see above) (considering there is not a transport limitation). This is also in good agreement with the XPS results (Table 1).

3.3.1. Optimization of the pH

The pH of the sample is one of the most important factors to consider for free chlorine determination in real samples. In general, the pH of waters containing free chlorine is in the range of 5 to 9 [20]. However, the decomposition of sodium hypochlorite is minimized in basic conditions, as the dissociation constant of HClO is 3.98×10^{-8} at 25 °C ($pK_a = 7.4$). It is then possible that hypochlorite ion coexists with hypochlorous acid within this pH range. The ratio of ClO^-:HOCl is calculated to be 2:98 at pH 5.8. However, at higher pH values (pH > 8.5) almost all the chlorine is present as ClO^-. The concentration of Cl_2 in the stock NaClO solution (13 ~ 14%, w/w) can be calculated as 2×10^{-10} mol/L, and as a result negligible for the following analysis.

With the aim of determining the influence of the pH on the free chlorine analysis, experiments were performed at three pH values, *i.e.* pH 5.8, 8 and 9. The selected pH range covers the typical conditions of water samples in applications targeted herein (*vide supra*). Fig. 7 shows LSVs at inkjet printed silver electrodes in a 16 ppm free chlorine solution and in the different pH buffer solutions. As it can be seen, the highest sensitivity was obtained at pH 8, followed by pH 5.8 and finally pH 9 (SEM images for different pH values showed in Fig. A.1). On pH 5.8 only HClO species are present in the solution, while on pH 8 both HOCl and ClO^- species were present (at pH 8 $[HClO]/[ClO^-] = 0.251$). The latter means that the OCl^- species were more reactive and contributes to higher sensitivity. According to the pK_a higher pH values are more favorable for the presence of OCl^-, but at pH 9 the yield of the reaction between the electrode and free chlorine species is harmed by the formation of Ag_2O, which probably quickly passivates the electrode surface. XPS analysis also revealed that at pH 9, the atomic ratio of O/Ag to Cl/Ag in the formed film was higher than at pH 8 (pH 5.8 O/Ag = 0.24, Cl/Ag = 0.28; pH 8: O/Ag = 0.39, Cl/Ag = 0.28; pH 9: O/Ag = 2.48, Cl/Ag = 0.15) (Fig. B.1). This means that the formation of Ag_2O is

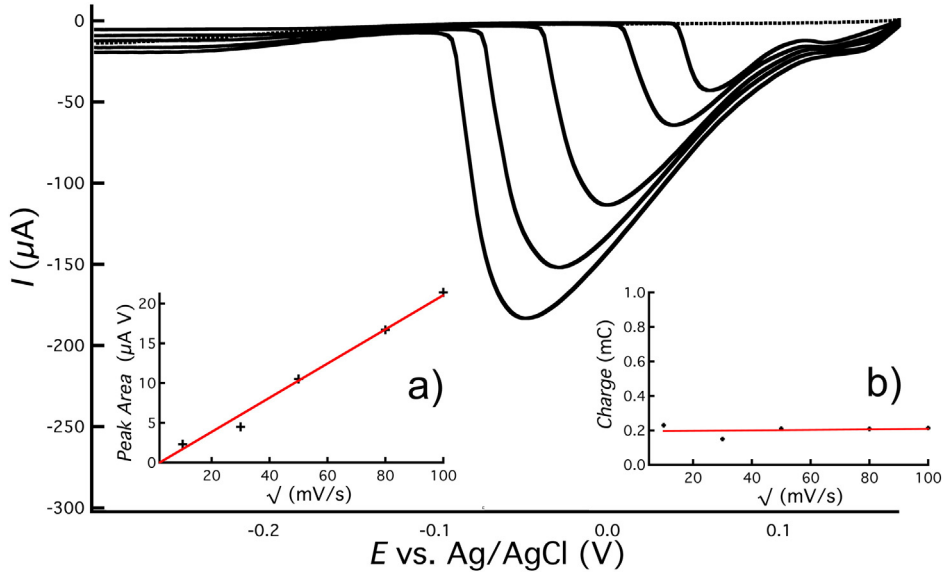

Fig. 6. Linear sweep voltammograms using an inkjet printed silver electrode in a 16 ppm free chlorine solution (50 mM KH_2PO_4, pH 5.8) (the dotted line represents the voltammogram in the absence of free chlorine species) at scan rates 10, 30, 50, 80 and 100 mV · s^{-1}. The inset plot a) represents the peak area against the scan rate (10–100 mV · s^{-1}), while inset b) is showing charge dependence on the same scan rate range. Preconditioning between each measurement for 15 s at −0.3 V, starting potential was 0.2 V and the reaction time with free chlorine was 60 s.

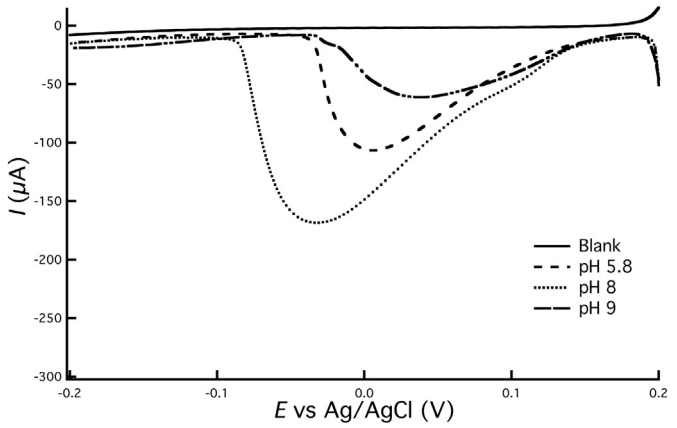

Fig. 7. Linear sweep voltammograms at an inkjet printed silver electrode in a 16 ppm free chlorine solution at different pH 5.8, 8, and 9. Preconditioning between each measurement for 15 s at −0.3 V, starting potential 0.2 V, reaction time with free chlorine 60 s, scan rate 100 mV · s^{-1}.

favored over AgCl at high pH values (also in agreement with the Pourbaix diagram for silver) and the more pronounced Ag_2O shoulder in the LSV at pH 9 [38]. Therefore, pH 8 was a good compromise with the highest sensitivity, so we used this value in further experiments.

3.3.2. Optimization of the Reaction Time

The formation of the AgCl/Ag_2O film depends also on the reaction time between the free chlorine and the silver electrode. As shown in Fig. 8, there is a clear increase of the peak current and peak area of the cathodic signal when the reaction time is increased. At reaction times equal or higher than 200 s, no further increase of the charge is observed due to a possible saturation of the electrode surface from the AgCl/Ag_2O formation. In addition, a vertical growth of the AgCl/Ag_2O could set in, resulting in the break off of nanoparticulate AgCl/Ag_2O during LSV scans that in consequence are not measured as charge. During the reaction time, it was also noticed that the open circuit potential (OCP) was changing and then reached a constant value, which was the same for different reaction times (30–500 s). For the experiment shown in Fig. 8, a sample containing 16 ppm free chlorine was employed. Therefore, a precise optimization of the experimental parameters must be performed depending on the targeted concentration range of free chlorine. The latter results demonstrate the feasibility of quantifying free chlorine in low concentrations by tuning the different parameters, such as the reaction time.

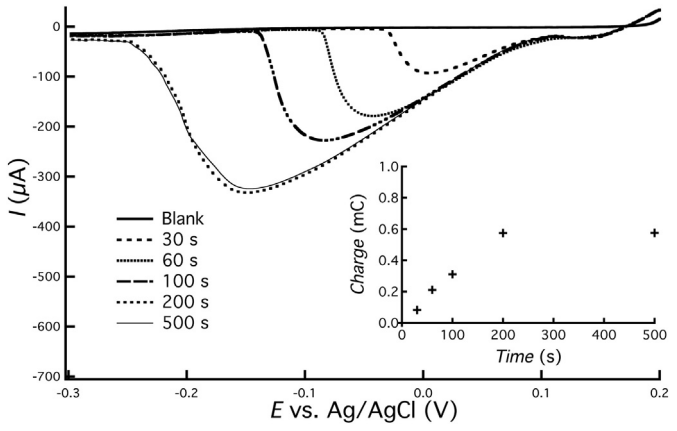

Fig. 8. Linear sweep voltammograms at an inkjet printed silver electrode in a 16 ppm of free chlorine solution with different reaction times: 30, 60, 100, 200 and 500 s. Preconditioning between each measurement = 15 s at −0.3 V, starting potential 0.2 V, scan rate 100 mV · s^{-1}. Inset plot represents charge against the reaction time.

3.3.3. Stability and Reproducibility Study

The stability of inkjet printed silver electrodes was verified by recording successive LSVs. The electrodes remained stable in a free chlorine solution for 3 consecutive analyses with a relative standard deviation (RSD, n = 3) of 3.6%. Afterwards small degradations of the silver structure (detaching from substrate) could be observed, which could not be fixed with the electrochemical preconditioning. This degradation was more important for higher free chlorine concentrations. However, electrodes could be used for at least 3 analyses, without any significant change in the voltammetric signal in the concentration range tested.

In order to demonstrate the reproducibility of the inkjet printing process, five electrodes from the same batch were employed to measure the same 16 ppm free chlorine solution (Fig. 9). It should be noticed that sodium hypochlorite solution could decompose fast during the measurement and cause slight variability in the obtained signal. A RSD (n = 5, each electrode tested in triplicate, calculated from the charge) of 7.6% was obtained confirming that inkjet printed silver electrodes can be used as disposable electrodes for the reproducible quantification of free chlorine in water.

3.3.4. Interferences

For the successful and selective determination of free chlorine in real field applications, the influence on the electrochemical signal of coexisting species was also studied. Special attention was paid on other species that could react with the silver electrode, forming for instance silver halides. With this aim, phosphate buffer solutions were spiked with hypobromite and hypoiodite, which upon reaction with silver electrode formed AgBr and AgI, respectively. The stripping potential of AgI and AgBr was equal to −0.25 V and 0.1 V, respectively (experimental values, depending on the concentration, Fig. C.1). Since the stripping potential for AgCl was around 0.2 V, (the maximum peak height potential depends on the free chlorine concentration) hypobromite and hypoiodite in high concentrations could cause the overlap of stripping signals. As for other halide species, we did not detect any influence on free chlorine determination.

3.3.5. Concentration Dependence Study

Fig. 10a shows the LSVs obtained in free chlorine solutions within a concentration range from 1 to 100 ppm under optimized conditions. With the increase of the free chlorine concentration, the reduction peak current significantly rises, demonstrating that the inkjet printed silver electrode is highly sensitive to the presence of free chlorine species. This is confirmed by the plot of the charge passed as a function of free chlorine concentration (Fig. 10b), where a clear linear trend can be found in the concentration range tested ($r^2 = 0.9940$). The slope of the current increase is constant for all AgCl concentrations due to the limited kinetics of the underlying electron-transfer processes. As a consequence, the complete reduction of the formed AgCl at the electrode surface is obtained at more negative potentials when the free chlorine concentration is higher. The error bars in Fig. 10b represent the standard deviation from triplicates experiments performed for each concentration tested. In the cases where error bars are not observable, it is because they are smaller than the data symbol employed. Sensitivity for free chlorine equal to 30 μC/ppm is extracted from the slope of the straight line of Fig. 10b. The lowest concentration of free chlorine calculated with standard addition method by extrapolating the calibration curve to $y = 0$ (x_E = a/b, where a is intercept of regression line and b is the slope; $y = 1.17 + 2.97\,x$) was 0.4 ppm, while limit of detection (S/N = 3) equal to 2 ppm, was calculated as LOD = 3 S_a/b, where S_a is the standard deviation of the intercept and b is the slope of the regression line. At higher free chlorine concentrations (>200 ppm), the electrode surface showed drastic damages on its structure and even a complete loss of the silver layer. Therefore, 200 ppm is the maximum concentration that can be tested with the present inkjet printed electrodes under the present conditions.

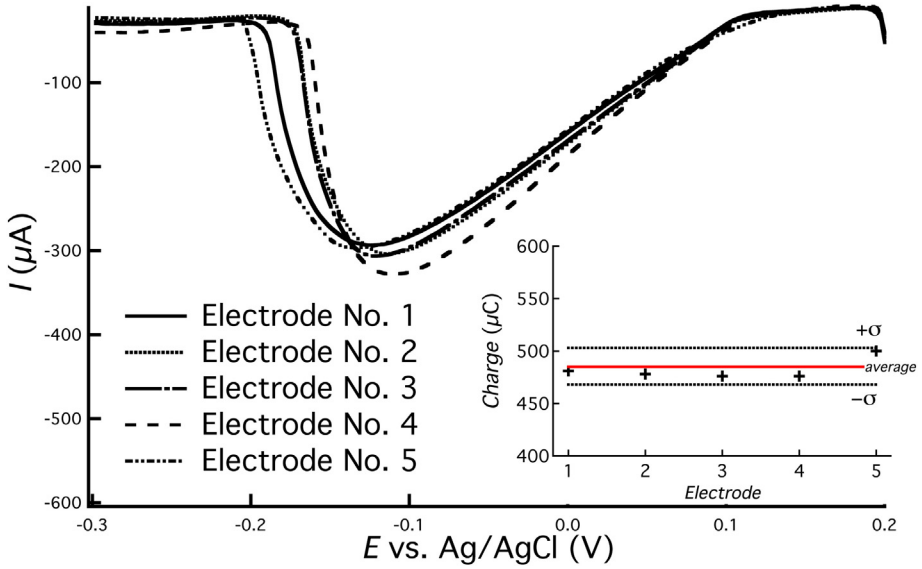

Fig. 9. Linear sweep voltammograms of different inkjet printed silver electrodes from the same batch in a 16 ppm free chlorine solution at pH 8. Preconditioning between each measurement for 15 s at −0.3 V, starting potential 0.2 V, reaction time with free chlorine 200 s, scan rate 100 mV s^{-1}. Inset plot represents charge variation for five different electrodes.

The high sensitivity and the linear response range of the proposed methodology makes it suitable for the analysis of swimming pool water, industrial water samples and even for forensic analysis.

3.4. Quantification of Free Chlorine in Real Water Samples

Finally, to validate the present methodology, several swimming pool samples were measured in parallel electrochemically and with the standard DPD colorimetric method (#330.5). The collected samples (from a public swimming pool in Lausanne, Switzerland) were spiked with two different concentrations of sodium hypochlorite. Table 2 shows the mean values of free chlorine concentration obtained with the two methods and each sample analyzed in triplicate. From the obtained results it is concluded that there is a good agreement between the present and the standard DPD methodologies. For both methods, the determined concentrations of free chlorine were lower than the initial one, probably due to fast free chlorine decomposition. Although the DPD method has a better sensitivity, the inkjet printed silver electrodes provide a fast, still sensitive and easy-to-perform analysis, without the need of external reagents. In order to validate the methodology with more concentrated samples, *Eau de Javel*, commonly used as disinfectant with 2.5% of sodium hypochlorite was diluted 250× and measured using the inkjet printed Ag electrode, which resulted in 98.78 ± 1.29 ppm. This confirms that the inkjet printed electrodes can be successfully used in the optimized range of free chlorine concentration. Furthermore, reproducible and disposable silver electrodes can be easily prepared by inkjet printing on a large scale and in any required geometry to fit on-line and on-site free chlorine analysis requirements.

4. Conclusion

Free chlorine detection at inkjet printed silver electrodes presents a simple, practical and precise technique, which is suitable for large-scale sensors production and can be implemented for environmental or industrial analyses. The main advantages of the present methodology are its simplicity, high reproducibility, sensitivity and the possibility to reuse the sensors (at least for three consecutive analyses) by simply implementing an electrochemical preconditioning step before each measurement. Silver electrodes were printed on a polyimide substrate, leading to a small, flexible, and portable sensor system. After optimization of different electrochemical parameters lowest concentration of free chlorine that could be detected from extrapolation of regression line to $y = 0$ was equal to 0.4 ppm (LOD equal to 2 ppm), which is appropriate for quantifying the maximum residual disinfectant level (MRDL) in water samples (*i.e.* 4 ppm). Additionally, a linear range from 1 to 100 ppm and a sensitivity of 30 μC/ppm were obtained. Finally,

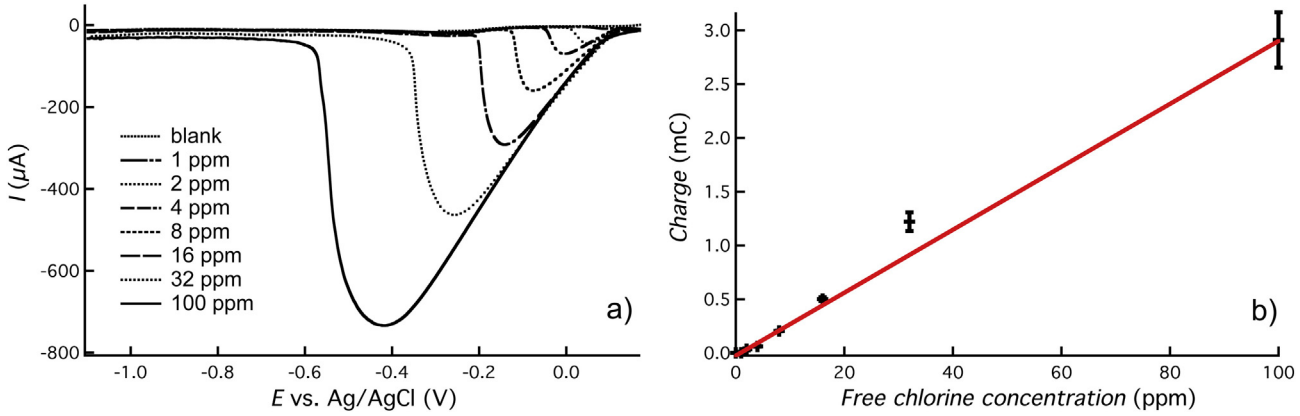

Fig. 10. a) Linear sweep voltammograms of an inkjet printed silver electrode in different concentrations of NaClO solutions at pH 8. b) Charge as a function of the concentration of free chlorine. Preconditioning between each measurement for 15 s at −0.3 V, starting potential 0.1 V, reaction time with free chlorine 200 s, scan rate 100 mV · s^{-1}. The error bars represent the standard deviation for a triplicate (at low concentration values, the error bars are smaller than the data symbol employed).

Table 2
Results of the recovery test of free chlorine in swimming pool water samples analyzed by the standard DPD method and the inkjet printed silver electrodes.

Spiked concentration	DPD method	Inkjet printed silver electrode
0 ppm	0.26 ± 0.03 ppm	Not detected
2 ppm	1.62 ± 0.05 ppm	1.81 ± 0.12 ppm
4 ppm	2.79 ± 0.04 ppm	3.02 ± 0.04 ppm

the present study serves as an example for implementing reliable and non-expensive inkjet printed strategies for the electrochemical quantification of environmentally relevant species based on silver electrodes.

Acknowledgment

The financial support of this research provided by the NanoTera program through the Envirobot Project is acknowledged.

Appendix A. Supplementary Data

Supplementary data to this article can be found online at http://dx.doi.org/10.1016/j.jelechem.2015.08.024.

References

[1] K. Wakigawa, A. Gohda, S. Fukushima, T. Mori, T. Niidome, Y. Katayama, Talanta 103 (2013) 81–85.
[2] B. Saad, W.T. Wai, S. Jab, W.S.W. Ngah, M.I. Saleh, J.M. Slater, Anal. Chim. Acta 537 (2005) 197–206.
[3] L.S. Clescerl, A.E. Greenberg, A.D. Eaton, American Public Health Association, 1999.
[4] Chlorine Residual Testing Fact Sheet, CDC SWS Project.
[5] J. Xu, K. Feng, M. Weck, Sensors Actuators B 156 (2011) 812–819.
[6] K. Cui, D. Zhang, G. Zhang, D. Zhu, Tetrahedron Lett. 51 (2010) 6052–6055.
[7] D.I. Pattison, M.J. Davies, Biochemistry 45 (2006) 8152–8162.
[8] D.I. Pattison, M.J. Davies, Chem. Res. Toxicol. 14 (2001) 1453–1464.
[9] S. Zierler, R.A. Danley, L. Feingold, Environ. Health Perspect. 69 (1986) 275.
[10] Fact sheet for NPDES general permit water treatment plants – wastewater discharge.
[11] General Permits Under the National Pollutant Discharge Elimination System (NPDES) for Certain POTWs and Other Treatment Works Treating Domestic Sewage in Massachusetts and New Hampshire and Indian Country Lands in Massachusetts.
[12] W.R. Melchert, D.R. Oliveira, F.R.P. Rocha, Microchem. J. 96 (2010) 77–81.
[13] M. Szili, I. Kasik, V. Matejec, G. Nagy, B. Kovacs, Sensors Actuators B 192 (2014) 92–98.
[14] S. Beutel, S. Henkel, Appl. Microbiol. Biotechnol. 91 (2011) 1493–1505.
[15] F. Kodera, M. Umeda, A. Yamada, Anal. Chim. Acta 537 (2005) 293–298.
[16] K.A.S. Pathiratne, S.S. Skandaraja, E.M.C.M. Jayasena, J. Natl. Sci. Found. Sri Lanka 36 (2008) 25–31.
[17] F. Kodera, M. Umeda, A. Yamada, Jpn. J. Appl. Phys. 2 Lett. Express Lett. 44 (2005) L718–L719.
[18] S.Y. Kishioka, T. Kosugi, A. Yamada, Electroanalysis 17 (2005) 724–726.
[19] O. Ordeig, R. Mas, J. Gonzalo, F.J. Del Campo, F.J. Munoz, C. de Haro, Electroanalysis 17 (2005) 1641–1648.
[20] M. Murata, T.A. Ivandini, M. Shibata, S. Nomura, A. Fujishima, Y. Einaga, J. Electroanal. Chem. 612 (2008) 29–36.
[21] R. Olivé-Monllau, A. Pereira, J. Bartrolí, M. Baeza, F. Céspedes, Talanta 81 (2010) 1593–1598.
[22] R. Olivé-Monllau, C.S. Martínez-Cisneros, J. Bartrolí, M. Baeza, F. Céspedes, Sensors Actuators B 151 (2011) 416–422.
[23] F.J. Del Campo, O. Ordeig, F.J. Munoz, Anal. Chim. Acta 554 (2005) 98–104.
[24] F. Kodera, S. Kishioka, M. Umeda, A. Yamada, Jpn. J. Appl. Phys. 43 (2004) L913–L914.
[25] F. Kodera, M. Umeda, A. Yamada, Bunseki Kagaku 54 (2005) 997–1002.
[26] J.Y. Jin, Y. Suzuki, N. Ishikawa, T. Takeuchi, Anal. Sci. 20 (2004) 205–207.
[27] S. Saputro, K. Takehara, K. Yoshimura, S. Matsuoka, Narsito, Electroanalysis 22 (2010) 2765–2768.
[28] K. Senthilkumar, J.-M. Zen, Electrochem. Commun. 46 (2014) 87–90.
[29] T.-H. Tsai, K.-C. Lin, S.-M. Chen, Int. J. Electrochem. Sci. 6 (2011) 2672–2687.
[30] S. Thiagarajan, Z.Y. Wu, S.M. Chen, J. Electroanal. Chem. 661 (2011) 322–328.
[31] Mitsui Mining & Smelting Co Ltd.
[32] M. Singh, H.M. Haverinen, P. Dhagat, G.E. Jabbour, Adv. Mater. 22 (2010) 673–685.
[33] K. Crowley, A. Morrin, M. Smyth, A. Killard, R. Shepherd, M. in het Panhuis, G. Wallace, Sensors, 2008, IEEE 2008, pp. 13–16.
[34] Li, et al., Nanoscale Res. Lett. 8 (2013) 442.
[35] J. Perelaer, C.E. Hendriks, A.W.M. de Laat, U.S. Schubert, Nanotechnology 20 (2009) 165303.
[36] E.T.S.G. da Silva, S. Miserere, L.T. Kubota, A. Merkoçi, Anal. Chem. 86 (2014) 10531–10534.
[37] L. Lin, X. Bai, Pigm. Resin Technol. 33 (2004) 238–244.
[38] W.T. Thompson, M.H. Kaye, C.W. Bale, A.D. Pelton, Pourbaix Diagrams for Multielement Systems, Uhlig's Corrosion Handbook, Second Edition John Wiley & Sons, Inc., 2000.